

Lepton flavor physics at $\mu^+\mu^+$ colliders

Kåre Fridell^{1,2}, Ryuichiro Kitano^{1,3}, and Ryoto Takai^{1,3}

¹*KEK Theory Center, Tsukuba 305-0801, Japan*

²*Department of Physics, Florida State University, Tallahassee, FL 32306, USA*

³*Graduate University for Advanced Studies (Sokendai), Tsukuba 305-0801, Japan*

Abstract

We discuss sensitivities to lepton flavor violating (and conserving) interactions at future muon colliders, especially at $\mu^+\mu^+$ colliders. Compared with the searches for rare decays of μ and τ , we find that the TeV-scale future colliders have better sensitivities depending on the pattern of hierarchy in the flavor mixings. As an example, we study the case with the type-II seesaw model, where the flavor mixing parameters have direct relation to the neutrino mass matrix. At a $\mu^+\mu^+$ collider, the number of events of the $\mu^+\mu^+ \rightarrow \mu^+\tau^+$ process can be larger than $\mathcal{O}(100)$ with the center of mass energy $\sqrt{s} = 2$ TeV, and with an integrated luminosity $\mathcal{L} = 1$ ab⁻¹, while satisfying bounds from rare decays of μ and τ . We discuss impacts of the overall mass scale of neutrinos as well as CP violating phases to the number of expected events.

Contents

1	Introduction	2
2	Model-independent analysis	4
3	Measuring the flavor structure at muon colliders	7
3.1	Type-II Seesaw Model	7
3.2	Signal rates	10
3.3	Elastic scattering	13
3.4	Ratios of cross sections	14
4	Summary	17

1 Introduction

The muon collider has been discussed as one of the possible future energy frontier experiments [1–6]. It is a quite exciting possibility that humans can reach up to $\mathcal{O}(10)$ TeV physics with an experiment of a reasonable size by using beams of artificially made unstable elementary particles. The ways to realize narrow enough muon beams for particle physics experiments have been extensively studied [7], and there is a possibility of realizing a $\mathcal{O}(\text{few})$ to $\mathcal{O}(10)$ TeV scale collider within reasonable time scale, such as in the next 20–30 years.

Besides precision tests of Standard Model (SM) [8] parameters, one of the most interesting physics goals at such high energy muon colliders would be the search for new particles with TeV scale masses. Observation of such particles would give direct information of beyond Standard Model (BSM) physics. On the other hand, at high energy colliders one can also look for new interactions among SM particles. Microscopic new physics (NP) effects can generically leave imprints of its existence in the effective operators of low energy physics. Such effects grow larger at high energy, enabling an efficient search at high-energy colliders such as a muon collider. In fact, the clean environment of lepton colliders is particularly beneficial for searches for such new interactions. For example, it has been demonstrated that precision measurements of $\sqrt{s} = 2$ TeV $\mu^+\mu^+$ elastic scatterings can probe physics at $\mathcal{O}(100)$ TeV [9].

It is interesting to note that $\mu^+\mu^+$ colliders may be constructed based on different technology than $\mu^+\mu^-$ colliders in terms of muon cooling [5, 10]. There is an established technology for a low

emittance μ^+ beam by using laser ionization of Muonium [7], which is the core technology of the muon $g-2$ /EDM experiment at J-PARC [11]. By scaling up this technology, there could be a scenario in which a $\mu^+\mu^+$ collider is realized much earlier than $\mu^+\mu^-$ colliders. Furthermore, the existing μ^+ cooling technology is in principle compatible with establishing a definite polarization of the μ^+ beam, which is also great advantage in distinguishing different NP models [12].

One definitive sign of NP at lepton colliders would be the potential observation of charged lepton flavor violation (LFV) [13]. There are existing bounds on LFV interactions coming from searches for rare muon and τ decays. Roughly speaking, the experimental limits are set by numbers of μ and τ such as 10^{13} and 10^8 at PSI and B -factories, respectively, which translates into $\mathcal{O}(100)$ and $\mathcal{O}(10)$ TeV scales for LFV interactions, respectively.

Previous works have focused on studying LFV in the context of specific models that involve e.g. a neutral scalar field or the type-I [14, 15], -II [16, 17], or -III [18] seesaw mechanisms at same- or opposite-sign lepton colliders. In Refs. [19, 20] the phenomenology of the type-I seesaw model was studied in the context of future muon colliders. The type-II seesaw was studied in Refs. [21–26] for opposite sign lepton colliders and in Ref. [27] for a same sign electron collider. In Refs. [28, 29] the authors studied the distinguishability of different seesaw types at lepton colliders, and in Ref. [30] LFV cross sections at same-sign muon colliders for different types of models were analyzed. Previous works have also focused on lepton number violation (LNV) in electron colliders via e.g. an inverse neutrinoless double beta decay process [31–34]. In fact, extensions of the SM by singly or doubly charged scalars with leptonic interactions can lead to signals of LNV as well as LFV at both lepton- [35–39] and hadron colliders [40–42], and they can be produced on-shell in opposite- or same-sign lepton colliders, respectively, so long as their mass is lower than the center-of-mass energy. For higher masses the LNV interactions could be studied in effective operators. However, severe constraints on such processes [43, 44] suggest that LNV interactions might be difficult to probe beyond current constraints.

In this paper, we study LFV scattering processes at future muon colliders, such as $\mu^+\mu^+ \rightarrow \mu^+\tau^+$, and estimate the experimental sensitivities to LFV interactions. We first study the effective interactions of LFV dimension-6 four-fermion operators, which could arise in models that induce LFV but do not necessarily correspond to a neutrino mass generation mechanism. As a reference model, we then consider the type-II seesaw model, for which the flavor structure of the operators is proportional to square of the neutrino mass matrix. This approach also leads to an effective comparison between collider processes and rare μ and τ decays that can be mediated by the same operators [45]. Furthermore, in our model example of the type-II seesaw, the relative size of the cross section for different LFV processes $\mu^+\mu^+ \rightarrow l^+\tau^+$, with $l = e, \mu$, and τ , will depend on the specific

structure of the neutrino mass matrix, including CP violating phases. Combining this knowledge with measurements of the neutrino oscillation parameters, we show how a potential observation of LFV at muon colliders may be able to confirm the microscopic origin of neutrino masses. Lastly we consider elastic $\mu^+\mu^+ \rightarrow \mu^+\mu^+$ interactions and the possibility to distinguish new interactions from those of the SM.

Compared with the existing limits on LFV interactions from rare lepton decays, we find that a 2 TeV muon collider can be a more sensitive probe of LFV interactions, depending on flavor structure of the underlying process. For a 10 TeV $\mu^+\mu^+$ collider we find that the sensitivity in probing the existence of LFV interactions is significantly better than any past searches for rare μ or τ decays. We also find that for purely left- or right-handed interactions the reach is better at $\mu^+\mu^+$ colliders than $\mu^+\mu^-$ simply due to the different contractions of flavor indices.

This paper is organized as follows. In Sec. 2 we discuss model independent LFV interactions at future muon colliders and compare our results with constraints from rare μ and τ decays. In Sec. 3 we then study the type-II seesaw model and its phenomenology at future muon colliders, and show how the relative cross sections for different LFV processes depend on the details of the neutrino mass matrix. Finally, we conclude in Sec. 4.

2 Model-independent analysis

We start with the study of effective four-fermion operators added to the SM Lagrangian,

$$\mathcal{L}_{\text{int}} = C_{AB}^{ijkl} (\bar{\ell}_i \gamma_\rho P_A \ell_j) (\bar{\ell}_k \gamma^\rho P_B \ell_l) + \text{h.c.}, \quad (1)$$

where A and B stand for the chirality projection, L or R , and i, j, k , and l are indices of charged lepton flavors, e, μ , and τ .

We first focus on $\tau - \mu$ flavor transitions via the operator with coefficient $C_{AB}^{\tau\mu\mu\mu}$, which can lead to LFV processes such as $\mu^+\mu^+ \rightarrow \mu^+\tau^+$ at muon colliders and $\tau \rightarrow 3\mu$ decay at B -factories. The cross section and the branching ratio (BR) of these processes are respectively given by

$$\sigma(\mu^+\mu^+ \rightarrow \mu^+\tau^+) = \frac{s}{4\pi} \left[|C_{LL}|^2 + |C_{RR}|^2 + \frac{1}{6} (|C_{LR}|^2 + |C_{RL}|^2) \right] \quad (2)$$

and

$$\text{BR}(\tau \rightarrow 3\mu) = \frac{\text{BR}(\tau \rightarrow e\nu\bar{\nu})}{4G_F^2} \left[|C_{LL}|^2 + |C_{RR}|^2 + \frac{1}{2} (|C_{LR}|^2 + |C_{RL}|^2) \right]. \quad (3)$$

Here \sqrt{s} is the center-of-mass energy and G_F is the Fermi constant. In Eqs. (2) and (3), and in the following discussion below, the flavor indices $\tau\mu\mu\mu$ are omitted for simplicity. The currently most

stringent experimental bound for the latter process is given by $\text{BR}(\tau \rightarrow 3\mu) < 2.1 \times 10^{-8}$, as obtained by the Belle collaboration [46].

The number of events expected at muon colliders is given by $N := \mathcal{L} \times \sigma(\mu^+ \mu^+ \rightarrow \mu^+ \tau^+)$, where \mathcal{L} is the integrated luminosity. For example, in the model with $C_{LL} = 1/\Lambda^2$ and with other coefficients vanishing, the number of events are expressed as

$$N = 100 \left(\frac{\Lambda}{33 \text{ TeV}} \right)^{-4} \left(\frac{\sqrt{s}}{2 \text{ TeV}} \right)^2 \left(\frac{\mathcal{L}}{1 \text{ ab}^{-1}} \right). \quad (4)$$

We see that the muon collider at $\sqrt{s} = 2 \text{ TeV}$ can probe physics at or above $\mathcal{O}(10) \text{ TeV}$. To directly compare the muon collider process with rare τ decays, we can also express N as

$$N = 7.9 \times 10^3 \xi_{\tau \rightarrow 3\mu} \left(\frac{\sqrt{s}}{2 \text{ TeV}} \right)^2 \left(\frac{\mathcal{L}}{1 \text{ ab}^{-1}} \right) \left(\frac{\text{BR}(\tau \rightarrow 3\mu)}{2.1 \times 10^{-8}} \right), \quad (5)$$

where

$$\xi_{\tau \rightarrow 3\mu} := \frac{|C_{LL}|^2 + |C_{RR}|^2 + \frac{1}{6}(|C_{LR}|^2 + |C_{RL}|^2)}{|C_{LL}|^2 + |C_{RR}|^2 + \frac{1}{2}(|C_{LR}|^2 + |C_{RL}|^2)} \quad (6)$$

is an $\mathcal{O}(1)$ quantity specified by the underlying theory. The expected number of events, $N = 7900$, should be large enough to be discovered at the reference energy and luminosity, $\sqrt{s} = 2 \text{ TeV}$ and $\mathcal{L} = 1 \text{ ab}^{-1}$, in the case where $\text{BR}(\tau \rightarrow 3\mu)$ is just below the experimental bound. The future sensitivity to the $\tau \rightarrow 3\mu$ branching ratio has been reported by the Belle II collaboration to be as low as $\text{BR}(\tau \rightarrow 3\mu) < 3.5 \times 10^{-10}$ [47]. For this value, the numerical factor in Eq. (5) is reduced to 130, which should be still large enough to potentially be discovered. This demonstrates that, even at a relatively low energy, future $\mu^+ \mu^+$ colliders are a powerful tool to look for LFV interactions.

At $\mu^+ \mu^-$ colliders, one can look for $\mu^+ \mu^- \rightarrow \mu^+ \tau^-$ and $\mu^+ \mu^- \rightarrow \tau^+ \mu^-$ events, which are induced by the same operator as discussed above. It turns out that the ratio of the number of events at $\mu^+ \mu^+$ and $\mu^+ \mu^-$ colliders is given by

$$\frac{\sigma(\mu^+ \mu^+ \rightarrow \mu^+ \tau^+)}{\sigma(\mu^+ \mu^- \rightarrow \mu^+ \tau^-) + \sigma(\mu^+ \mu^- \rightarrow \tau^+ \mu^-)} = \frac{3}{2} \times \frac{|C_{LL}|^2 + |C_{RR}|^2 + \frac{1}{6}(|C_{LR}|^2 + |C_{RL}|^2)}{|C_{LL}|^2 + |C_{RR}|^2 + |C_{LR}|^2 + |C_{RL}|^2}. \quad (7)$$

For the model with $C_{LL} \neq 0$, for example, the sensitivity is better at $\mu^+ \mu^+$ colliders than $\mu^+ \mu^-$. Furthermore, the polarizability of the μ^+ beam will also enhance the signal rate.

Generally, the LFV $\mu - e$ transition is more stringently constrained than any LFV process that involves the τ sector. In order to compare the expected signal rate of $\mu^+ \mu^+ \rightarrow \mu^+ \tau^+$ with the constraint from rare muon decays, we need to parameterize the flavor hierarchy in the coefficients C_{AB}^{ijkl} . The strongest bound is obtained from $\mu \rightarrow 3e$ decays via $C_{AB}^{\mu e e e}$ with $\text{BR}(\mu \rightarrow 3e) < 1.0 \times 10^{-12}$ [48]. Normalizing with this bound, the expected number of events at a muon collider are estimated to be

$$N = 6.7 \times 10^{-2} \xi_{\mu \rightarrow 3e} \left(\frac{\sqrt{s}}{2 \text{ TeV}} \right)^2 \left(\frac{\mathcal{L}}{1 \text{ ab}^{-1}} \right) \left(\frac{\text{BR}(\mu \rightarrow 3e)}{1.2 \times 10^{-12}} \right), \quad (8)$$

Process	Current BR limit	$N(\mu^+\mu^+ \rightarrow \mu^+\tau^+)$	Future BR limit	$N(\mu^+\mu^+ \rightarrow \mu^+\tau^+)$
$\mu \rightarrow 3e$	$< 1.0 \times 10^{-12}$ [48]	$< 6.7 \times 10^{-2}$	$\sim 10^{-16}$ [49]	$\sim 7 \times 10^{-6}$
$\tau \rightarrow 3e$	$< 2.7 \times 10^{-8}$ [46]	$< 1.0 \times 10^4$	$\sim 5 \times 10^{-10}$ [47]	~ 190
$\tau \rightarrow \mu^+\mu^-e^-$	$< 2.7 \times 10^{-8}$ [46]	$< 1.0 \times 10^4$	$\sim 4.5 \times 10^{-10}$ [47]	~ 170
$\tau \rightarrow e^+\mu^-\mu^-$	$< 1.7 \times 10^{-8}$ [46]	$< 6.4 \times 10^3$	$\sim 2.5 \times 10^{-10}$ [47]	~ 95
$\tau \rightarrow e^+e^-\mu^-$	$< 1.8 \times 10^{-8}$ [46]	$< 6.8 \times 10^3$	$\sim 3 \times 10^{-10}$ [47]	~ 110
$\tau \rightarrow \mu^+e^-e^-$	$< 1.5 \times 10^{-8}$ [46]	$< 5.7 \times 10^3$	$\sim 2.2 \times 10^{-10}$ [47]	~ 83
$\tau \rightarrow 3\mu$	$< 2.1 \times 10^{-8}$ [46]	$< 7.9 \times 10^3$	$\sim 3.5 \times 10^{-10}$ [47]	~ 130

Table 1: The upper bounds on the number of $\mu^+\mu^+ \rightarrow \mu^+\tau^+$ events at a $\mu^+\mu^+$ collider with $\sqrt{s} = 2$ TeV and $\mathcal{L} = 1$ ab $^{-1}$ corresponding to the experimental bounds on rare μ or τ decays. We take the flavor mixing to be universal, i.e. we assume no flavor hierarchy in the effective operators, such that $\xi_{\ell_i \rightarrow \ell_j \ell_k \ell_l} = 1$. In the fourth and fifth columns, the future sensitivities on the BR of each LFV decay process and corresponding number of events at a $\mu^+\mu^+$ collider are shown, respectively. As a second benchmark scenario, we note that for a muon collider with $\sqrt{s} = 10$ TeV and $\mathcal{L} = 10$ ab $^{-1}$, each event number should be multiplied by a factor 250.

where

$$\xi_{\mu \rightarrow 3e} := \frac{|C_{LL}^{\tau\mu\mu\mu}|^2 + |C_{RR}^{\tau\mu\mu\mu}|^2 + \frac{1}{6}(|C_{LR}^{\tau\mu\mu\mu}|^2 + |C_{RL}^{\tau\mu\mu\mu}|^2)}{|C_{LL}^{\mu e e e}|^2 + |C_{RR}^{\mu e e e}|^2 + \frac{1}{2}(|C_{LR}^{\mu e e e}|^2 + |C_{RL}^{\mu e e e}|^2)}. \quad (9)$$

The number of events, N , can be as large as 100 at $\sqrt{s} = 2$ TeV and $\mathcal{L} = 1$ ab $^{-1}$ if $\sqrt{\xi_{\mu \rightarrow 3e}} \gtrsim 40$. For example, as we will discuss below, the $\sqrt{\xi_{\mu \rightarrow 3e}}$ parameter is as large as $\Delta m_{\text{atm}}^2 / \Delta m_{\text{sol}}^2 \sim 30$ in the model where the effective operator is related to the mechanism to generate the neutrino masses, and can potentially be larger depending on the specific structure of the neutrino mass matrix. We therefore see that there is a possibility of finding LFV processes at a $\mu^+\mu^+$ collider even under strong constraints from rare decays.

For completeness, we list number of events corresponding to the μ and τ decays in Table 1, where we take the ξ parameter defined as

$$\xi_{\ell_i \rightarrow \ell_j^+ \ell_k^- \ell_l^-} := \frac{|C_{LL}^{\tau\mu\mu\mu}|^2 + |C_{RR}^{\tau\mu\mu\mu}|^2 + \frac{1}{6}(|C_{LR}^{\tau\mu\mu\mu}|^2 + |C_{RL}^{\tau\mu\mu\mu}|^2)}{\frac{1}{2} \left[|C_{LL}^{ijkl}|^2 + |C_{RR}^{ijkl}|^2 + \frac{1}{1+\delta_{kl}} (|C_{LR}^{ijkl}|^2 + |C_{RL}^{ijkl}|^2) \right] + (k \leftrightarrow l)} \quad (10)$$

as unity. If we take the coefficients with the different flavor indices as independent free parameters, the muon colliders offer a unique way to test the $C_{AB}^{\mu\mu\mu\mu}$ and $C_{AB}^{\mu\mu\tau\tau}$ interactions, as these operators cannot be probed by rare μ or τ decays.

3 Measuring the flavor structure at muon colliders

As a concrete model example that realizes the effective operator analysis of the previous section, we consider the type-II seesaw model, which generates LFV four-fermion operators at tree level. The Wilson coefficients have direct relations to the neutrino mass matrix, and thus the model can be tested by comparing results from $\mu^+\mu^+$ colliders with neutrino oscillation data. We also discuss the importance of CP violating phases in the LFV scattering processes.

3.1 Type-II Seesaw Model

In the type-II seesaw model, the SM is extended by a Higgs triplet field

$$\Delta = \begin{pmatrix} \Delta^+/\sqrt{2} & \Delta^{++} \\ \Delta^0 & -\Delta^+/\sqrt{2} \end{pmatrix} \quad (11)$$

which has a hypercharge $Y = 2$. The Yukawa interactions between the left-handed lepton fields L_i are introduced as

$$\mathcal{L}_{\text{type-II}} \supset h_{ij} \bar{L}_i^c i\sigma^2 \Delta L_j + \text{h.c.}, \quad (12)$$

where i, j are the flavor indices, h_{ij} is a 3×3 symmetric coupling matrix, and σ^2 is the second Pauli matrix to contract the $SU(2)_L$ indices. Upon $SU(2)_L$ symmetry breaking, the neutrino mass term

$$\mathcal{L}_\nu = h_{ij} \frac{v_\Delta}{\sqrt{2}} \bar{\nu}_i^c P_L \nu_j + \text{h.c.} = \frac{1}{2} m_{ij} \bar{\nu}_i^c P_L \nu_j + \text{h.c.} \quad (13)$$

is obtained from Eq. (12), where v_Δ is the vacuum expectation value (VEV) of the neutral component of the Higgs triplet, i.e. $\langle \Delta^0 \rangle = v_\Delta/\sqrt{2}$. This VEV spontaneously breaks $B - L$ symmetry and leads to Majorana masses for the neutrinos. The neutrino mass matrix $m_{ij} = \sqrt{2}v_\Delta h_{ij}$ can then be diagonalized as

$$m = U \hat{m}_\nu U^T, \quad (14)$$

where $\hat{m}_\nu = \text{diag}(m_1, m_2, m_3)$ is the diagonal neutrino mass matrix in the mass basis and U is the 3×3 Pontecorvo–Maki–Nakagawa–Sakata (PMNS) matrix. Including the two Majorana CP-violating phases ϕ_1 and ϕ_2 , as well as the Dirac CP-violating phase δ_{CP} , this matrix can be denoted as

$$U = \begin{pmatrix} c_{12}c_{13} & s_{12}c_{13} & s_{13}e^{-i\delta_{\text{CP}}} \\ -s_{12}c_{23} - c_{12}s_{23}s_{13}e^{i\delta_{\text{CP}}} & c_{12}c_{23} - s_{12}s_{23}s_{13}e^{i\delta_{\text{CP}}} & s_{23}c_{13} \\ s_{12}s_{23} - c_{12}c_{23}s_{13}e^{i\delta_{\text{CP}}} & -c_{12}s_{23} - s_{12}c_{23}s_{13}e^{i\delta_{\text{CP}}} & c_{23}c_{13} \end{pmatrix} \begin{pmatrix} e^{i\phi_1} & 0 & 0 \\ 0 & e^{i\phi_2} & 0 \\ 0 & 0 & 1 \end{pmatrix}, \quad (15)$$

where $s_{ij} = \sin \theta_{ij}$ and $c_{ij} = \cos \theta_{ij}$. Throughout this work we assume normal hierarchy for the neutrino masses. The extension to inverted hierarchy is straightforward, and in general, muon decays

Process	Experimental limit	Constraint on	Bound $\times (m_\Delta/\text{TeV})^2$
$\mu \rightarrow e\gamma$	$< 4.2 \times 10^{-13}$ [52]	$ (h^\dagger h)_{e\mu} $	$< 2.4 \times 10^{-4}$
$\mu \rightarrow 3e$	$< 1.0 \times 10^{-12}$ [48]	$ h_{\mu e} h_{ee} $	$< 2.3 \times 10^{-5}$
$\tau \rightarrow e\gamma$	$< 3.3 \times 10^{-8}$ [53]	$ (h^\dagger h)_{e\tau} $	$< 1.6 \times 10^{-1}$
$\tau \rightarrow \mu\gamma$	$< 4.2 \times 10^{-8}$ [54]	$ (h^\dagger h)_{\mu\tau} $	$< 1.9 \times 10^{-1}$
$\tau \rightarrow 3e$	$< 2.7 \times 10^{-8}$ [46]	$ h_{\tau e} h_{ee} $	$< 9.2 \times 10^{-3}$
$\tau \rightarrow \mu^+ \mu^- e^-$	$< 2.7 \times 10^{-8}$ [46]	$ h_{\tau\mu} h_{\mu e} $	$< 6.5 \times 10^{-3}$
$\tau \rightarrow e^+ \mu^- \mu^-$	$< 1.7 \times 10^{-8}$ [46]	$ h_{\tau e} h_{\mu\mu} $	$< 7.3 \times 10^{-3}$
$\tau \rightarrow e^+ e^- \mu^-$	$< 1.8 \times 10^{-8}$ [46]	$ h_{\tau e} h_{\mu e} $	$< 5.3 \times 10^{-3}$
$\tau \rightarrow \mu^+ e^- e^-$	$< 1.5 \times 10^{-8}$ [46]	$ h_{\tau\mu} h_{ee} $	$< 6.9 \times 10^{-3}$
$\tau \rightarrow 3\mu$	$< 2.1 \times 10^{-8}$ [46]	$ h_{\tau\mu} h_{\mu\mu} $	$< 8.1 \times 10^{-3}$
$M \rightarrow \bar{M}$	$\leq 8.2 \times 10^{-11}$ [55]	$ h_{ee} h_{\mu\mu} $	$< 4.9 \times 10^{-2}$

Table 2: Bounds on the Yukawa coupling constants at 90 % C.L. in the type-II seesaw model, where h_{ij} are the Yukawa couplings and m_Δ is the mass of the doubly charged Higgs Δ^{++} [56]. The experimental limits in the upper block are branching ratios of the processes and in the lower block is the limit on the probability of spontaneous muonium (M) to antimuonium (\bar{M}) conversion.

would give stronger bounds while the $\mu^+ \mu^+ \rightarrow e^+ \mu^+$ process gets more important than the final states with τ^+ compared to the case of the normal hierarchy.

Different constraints on the parameters of the type-II seesaw model come from the electroweak precision tests, LFV rare decays, as well as the direct searches of additional Higgs bosons at the LHC. The VEV of the neutral element of the Higgs triplet v_Δ has a 3σ upper bound [24]

$$v_\Delta \leq 2.6 \text{ GeV}, \quad (16)$$

from a global fit of the electroweak precision parameter ρ given by $\rho = 1.00038 \pm 0.00020$ [50]. In order to explain the neutrino masses of $\mathcal{O}(\text{eV})$ or lower, the h_{ij} coupling constants need to be larger than $\mathcal{O}(10^{-10})$ while $\mathcal{O}(1)$ couplings are consistent if v_Δ is very small. The LHC experiments put lower bounds on the mass of the doubly charged Higgs $m_\Delta > 1080 \text{ GeV}$ at 95 % C.L. for Yukawa couplings $h_{ij} = 0.02$ [51]. For a given mass of the doubly charged Higgs, the Yukawa couplings are also bounded by precise measurements of different LFV processes. Specifically, the couplings are constrained by decays of μ or τ leptons into lepton plus photon $\ell_i \rightarrow \ell_j \gamma$, or into three leptons $\ell_i \rightarrow \ell_j \ell_k \ell_l$, as well as the conversion of muonium to antimuonium. Out of these processes, $\mu \rightarrow e\gamma$ and $\mu \rightarrow 3e$ decays provide the most stringent constraints. Table 2 shows the limits on the Yukawa matrix from these types of experiments.

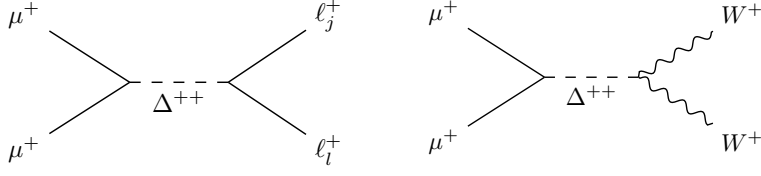


Figure 1: Diagrams showing LFV (left) and LNV (right) processes at a $\mu^+\mu^+$ collider involving the doubly charged scalar Δ^{++} from the type-II seesaw model.

The type-II seesaw model also leads to LNV processes such as

$$\ell_i^+ \ell_j^+ \rightarrow W^+ W^+ \quad (17)$$

as shown in Figure 1 (right), where i and j are flavor indices. The cross section for this process is given as

$$\sigma(\ell_i^+ \ell_j^+ \rightarrow W^+ W^+) = \frac{G_F^2 |m_{ij}|^2}{2\pi(1 + \delta_{ij})} \frac{(s - 2m_W^2)^2 + 8m_W^4}{(s - m_\Delta^2)^2 + m_\Delta^2 \Gamma_\Delta^2} \sqrt{1 - 4\frac{m_W^2}{s}}, \quad (18)$$

where G_F is the Fermi constant, δ_{ij} is the Kronecker's delta, and Γ_Δ is the width of Δ^{++} , given by

$$\Gamma_\Delta = \frac{G_F^2 v_\Delta^2}{2\pi m_\Delta} [(m_\Delta^2 - 2m_W^2)^2 + 8m_W^4] \sqrt{1 - 4\frac{m_W^2}{m_\Delta^2}} + \sum_{j,l} \frac{|h_{jl}|^2 m_\Delta}{4\pi(1 + \delta_{jl})}. \quad (19)$$

The branching ratio of the Higgs triplet into a pair of W bosons, which is determined by the first term in Eq. (19), is dominant in the large v_Δ region, while for small v_Δ the lepton number conserving decay of the triplet into a lepton pair dominates [24]. Here we have assumed that the branching ratios for the decays of the doubly charged Higgs triplet into other Higgs triplet particles is negligible compared to the decays into two leptons or two W bosons¹.

For the remainder of this work we focus on the processes

$$\mu^+ \mu^+ \rightarrow \ell_j^+ \ell_l^+ \quad (20)$$

mediated by a doubly charged Higgs boson, as illustrated in Figure 1 (left). This process violates conservation of charged lepton flavor unless $\ell_j = \ell_l = \mu$, and for small v_Δ it can dominate over the LNV process shown in Figure 1 (right). The cross section is given as

$$\sigma(\mu^+ \mu^+ \rightarrow \ell_j^+ \ell_l^+) = \frac{|h_{\mu\mu} h_{jl}|^2}{4\pi(1 + \delta_{jl})} \frac{s}{(s - m_\Delta^2)^2 + m_\Delta^2 \Gamma_\Delta^2}, \quad (21)$$

where we have treated the final state leptons as massless. Note that for $j = l = \mu$ there is an interference with the SM scattering, and Eq. (21) therefore does not correspond to the total cross section in this case. The cross section ratios

$$\frac{\sigma(\mu^+ \mu^+ \rightarrow \ell_j^+ \ell_l^+)}{\sigma(\mu^+ \mu^+ \rightarrow \ell_r^+ \ell_s^+)} = \frac{1 + \delta_{rs}}{1 + \delta_{jl}} \left| \frac{m_{jl}}{m_{rs}} \right|^2 \quad (22)$$

¹Note that for a small VEV $v_\Delta \ll v$ and large mass $m_\Delta \gg v$, where v is the VEV of the SM Higgs, the mass splitting between different components of the triplet Higgs Δ is small, such that this decay mode would be suppressed [56].

are particularly interesting observables as they provide information on the structure of the neutrino mass matrix, including the CP phases.

3.2 Signal rates

For $\sqrt{s} \ll m_\Delta$, we can integrate out the Δ bosons and are left with the dimension-6 effective operators in Eq. (1) with $A = B = L$. The LFV scattering processes $\mu^+ \mu^+ \rightarrow \ell_j^+ \ell_l^+$ can then be mediated by those operators. The Wilson coefficients are given by

$$C_{LL}^{\mu j \mu l} = \frac{h_{\mu\mu}^* h_{jl}}{m_\Delta^2}, \quad C_{LR}^{\mu j \mu l} = C_{RL}^{\mu j \mu l} = C_{RR}^{\mu j \mu l} = 0 \quad (23)$$

and the ξ parameter defined in Eq. (10) is then given by

$$\sqrt{\xi_{\ell_q^+ \rightarrow \ell_r^+ \ell_s^- \ell_t^-}} = \left| \frac{h_{\mu\mu} h_{jl}}{h_{qr} h_{st}} \right| = \left| \frac{m_{\mu\mu} m_{jl}}{m_{qr} m_{st}} \right|. \quad (24)$$

In order to get a sense of the number of events that are expected at muon colliders, we first parameterize the scale of the dimension-six operators Λ as

$$\frac{1}{\Lambda^2} := C_{LL}^{\tau\tau\tau\tau} \Big|_{m_1=0, \delta_{\text{CP}}=\phi_1=\phi_2=0} = \frac{|\bar{m}_{\tau\tau}|^2}{2m_\Delta^2 v_\Delta^2}. \quad (25)$$

Here \bar{m}_{ij} is a reference value which is defined as the (ij) component of the neutrino mass matrix in the flavor basis with the choices of a set of undetermined parameters by neutrino oscillation experiments, $m_1 = 0$ and $\delta_{\text{CP}} = \phi_1 = \phi_2 = 0$. The mass-squared differences and mixing angles in \bar{m}_{ij} are taken to be the central values from Ref. [57], which are explicitly given as

$$\begin{aligned} \theta_{12} &= 33.45^\circ, & \theta_{13} &= 8.62^\circ, & \theta_{23} &= 42.1^\circ, \\ \Delta m_{12}^2 &= 7.42 \times 10^{-5} \text{ eV}^2, & \Delta m_{13}^2 &= 2.517 \times 10^{-3} \text{ eV}^2. \end{aligned} \quad (26)$$

By using this scale Λ , the number of $\mu^+ \mu^+ \rightarrow \mu^+ \tau^+$ events can be expressed as

$$N(\mu^+ \mu^+ \rightarrow \mu^+ \tau^+) = 100 \left| \frac{m_{\mu\mu} m_{\mu\tau}}{\bar{m}_{\mu\mu} \bar{m}_{\mu\tau}} \right|^2 \left(\frac{\sqrt{s}}{2 \text{ TeV}} \right)^2 \left(\frac{\mathcal{L}}{1 \text{ ab}^{-1}} \right) \left(\frac{\Lambda}{34 \text{ TeV}} \right)^{-4}. \quad (27)$$

This demonstrates that, for the normal and hierarchical neutrino mass pattern with no CP violation, the scale to be probed at future $\mu^+ \mu^+$ colliders is $\mathcal{O}(30) \text{ TeV}$ at $\sqrt{s} = 2 \text{ TeV}$.

For comparison, we can express the branching ratios of the rare muon decay processes as

$$\text{BR}(\mu \rightarrow e\gamma) = 4.2 \times 10^{-13} \left| \frac{(m^\dagger m)_{e\mu}}{(\bar{m}^\dagger \bar{m})_{e\mu}} \right|^2 \left(\frac{\Lambda}{45 \text{ TeV}} \right)^{-4}, \quad (28)$$

and

$$\text{BR}(\mu \rightarrow 3e) = 1.0 \times 10^{-12} \left| \frac{m_{ee} m_{e\mu}}{\bar{m}_{ee} \bar{m}_{e\mu}} \right|^2 \left(\frac{\Lambda}{45 \text{ TeV}} \right)^{-4}. \quad (29)$$

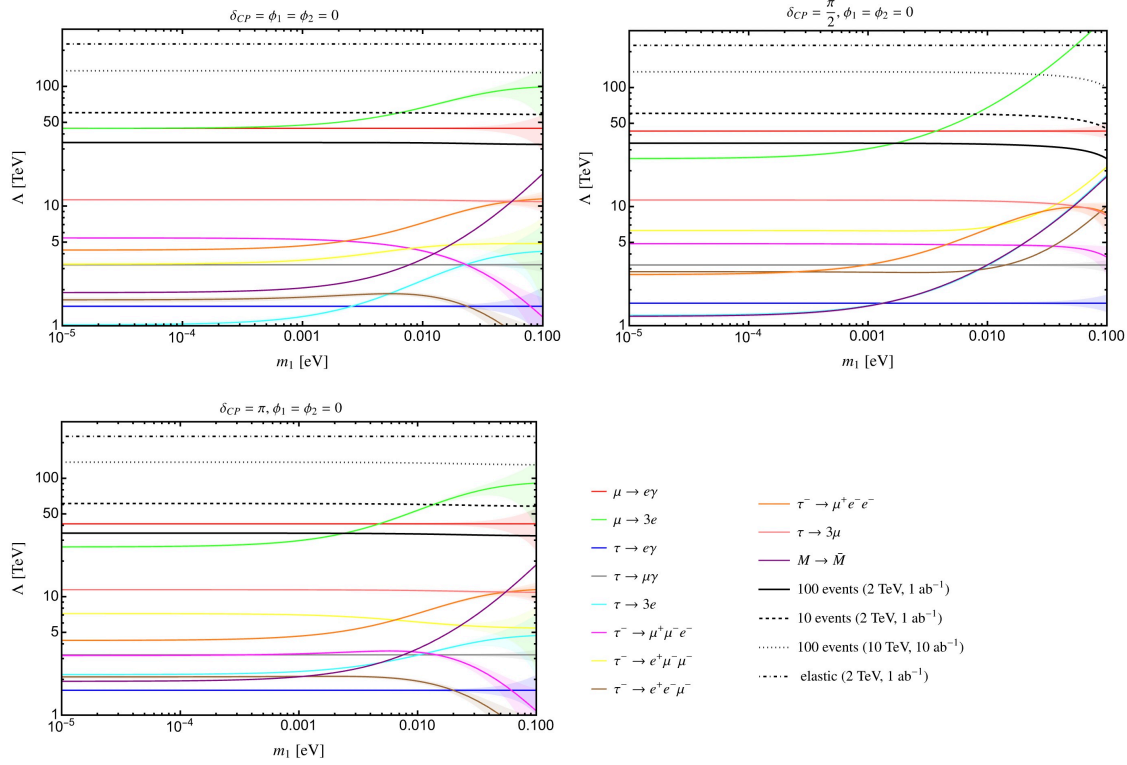


Figure 2: The constraint on the scale $\Lambda := \sqrt{2}m_\Delta v_\Delta/|\bar{m}_{\tau\tau}|$ as a function of the lightest neutrino mass m_1 , where \bar{m} is the neutrino mass matrix in the flavor basis with the CP-violating Majorana phases ϕ_1 and ϕ_2 set to 0, and the central values for the mixing angles and mass splittings given in Eq. (26). The CP-violating Dirac phase δ_{CP} set to 0 (top left), $\pi/2$ (top right), and π (bottom left). We find that the results are invariant for $\delta_{CP} \leftrightarrow -\delta_{CP}$. The solid colored lines show constraints coming from different LFV experiments, with regions below the lines being excluded. The black solid (dashed) lines represent the case that we observe 100 (10) $\mu^+\mu^+ \rightarrow \mu^+\tau^+$ events at muon colliders with $\sqrt{s} = 2$ TeV and $\mathcal{L} = 1$ ab^{-1} . The dotted lines show the case that $\sqrt{s} = 10$ TeV and $\mathcal{L} = 10$ ab^{-1} . Finally, the black dot-dashed lines show the potential discovery reach at muon colliders using elastic $\mu^+\mu^+ \rightarrow \mu^+\mu^+$ scattering. For all lines we consider the normal hierarchy ($m_1 < m_2 < m_3$) of neutrino masses. The shaded regions come from varying the neutrino mixing parameters within their 1σ limits.

Here the $\mu \rightarrow e\gamma$ process is mediated by a one-loop diagram with the Δ boson in the internal line [24]. We find that, with the reference neutrino masses, the experimental sensitivities in terms of Λ are similar to that of muon colliders at $\sqrt{s} = 2$ TeV.

In Figure 2 we compare the constraints on Λ coming from different LFV experiments with the potential reach at a future $\mu^+\mu^+$ collider, as a function of the lightest neutrino mass m_1 and for different values of the CP-violating Dirac phase δ_{CP} . We find that the results are invariant for $\delta_{CP} \leftrightarrow -\delta_{CP}$ if the CP-violating Majorana phases ϕ_1 and ϕ_2 are 0. For hierarchical neutrino masses, i.e. when m_1 goes to zero, the constraints from $\mu \rightarrow e\gamma$ and $\mu \rightarrow 3e$ decays corresponds to 10 – 100

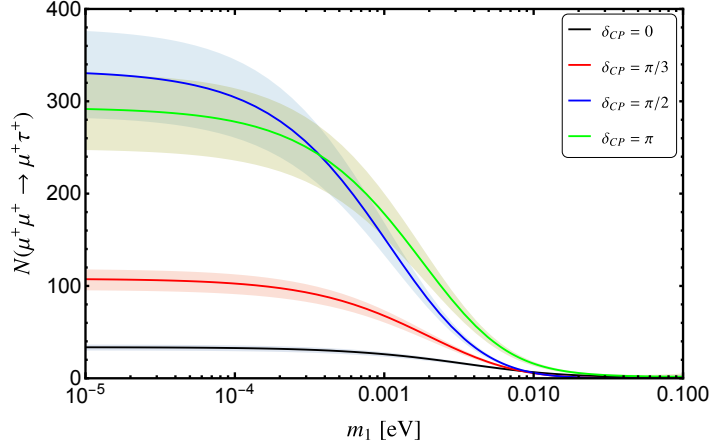


Figure 3: The number of $\mu^+\mu^+ \rightarrow \mu^+\tau^+$ events as a function of the lightest neutrino mass m_1 in the type-II seesaw model at a $\sqrt{s} = 2$ TeV, $\mathcal{L} = 1 \text{ ab}^{-1}$ muon collider, assuming that the couplings and masses of the triplet Higgs take values such that the branching ratio of the LFV $\mu \rightarrow 3e$ decay is right at the experimental limit $\text{BR}(\mu \rightarrow 3e) = 1.0 \times 10^{-12}$. The black, red, blue and green line represent the case that $\delta_{\text{CP}} = 0, \pi/3, \pi/2, \pi$. The neutrino mixing parameters $\theta_{12}, \theta_{23}, \theta_{13}, \Delta m_{21}^2$ and Δm_{31}^2 are taken from Ref. [57], and the Majorana CP phases are set as $\phi_1 = \phi_2 = 0$. The shaded regions come from varying the neutrino mixing parameters within their 1σ limits. We assume normal hierarchy ($m_1 < m_2 < m_3$) for the neutrino masses.

events at a $\mu^+\mu^+$ collider with $\sqrt{s} = 2$ TeV and $\mathcal{L} = 1 \text{ ab}^{-1}$, as can be seen from Figure 2. The constraint from $\mu \rightarrow 3e$ decay is more important for degenerate neutrino masses. For $\sqrt{s} = 10$ TeV and $\mathcal{L} = 10 \text{ ab}^{-1}$, the reach of $\mu^+\mu^+$ colliders is generally stronger than any existing LFV constraints for almost the whole range of m_1 .

The angular distribution of $\mu^+\mu^+ \rightarrow \mu^+\mu^+$ elastic scattering events can also be used to put constraints on the scale Λ [9], which is shown as the black dot-dashed line in Figure 2. As we discuss in the next subsection, this is a completely independent method from that of LFV searches since the NP contributions interfere with the SM amplitudes. The cross section therefore has $1/\Lambda^2$ contributions in contrast to the case for LFV processes, which only depend on $1/\Lambda^4$. Once we assume good angular resolutions of detectors and a precise theoretical calculation is done for the SM amplitudes, the reach is actually higher for elastic scattering than for LFV scattering processes. Therefore, it may be the case that a deviation from the SM is first observed in the elastic scattering, and the LFV processes, which give much clearer signs of NP, could then potentially be observed at higher luminosities.

The branching ratios of $\ell_i \rightarrow \ell_j \ell_k \ell_l$ depend strongly on the CP phases. In Figure 3, we show the number of events of the $\mu^+\mu^+ \rightarrow \mu^+\tau^+$ process at the $\sqrt{s} = 2$ TeV and $\mathcal{L} = 1 \text{ ab}^{-1}$ collider by taking the NP scale Λ to be equal to the experimental bounds coming from $\mu \rightarrow 3e$ decays, for several choices of δ_{CP} . Note that the variation for different values of δ_{CP} mainly comes from the variation in

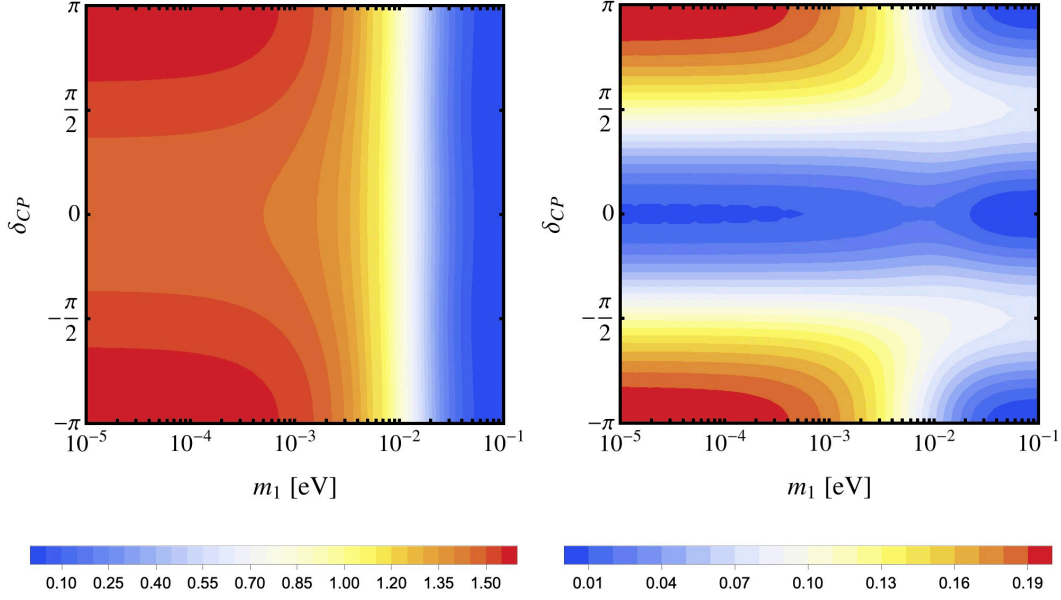


Figure 4: The ratio of cross sections, $\sigma(\mu^+\mu^+ \rightarrow \mu^+\tau^+)/\sigma(\mu^+\mu^+ \rightarrow \tau^+\tau^+)$ (left) and $\sigma(\mu^+\mu^+ \rightarrow e^+\tau^+)/\sigma(\mu^+\mu^+ \rightarrow \tau^+\tau^+)$ (right) as functions of the lightest neutrino mass m_1 and the Dirac CP phase δ_{CP} , for normal hierarchy ($m_1 < m_2 < m_3$) of neutrino masses. The neutrino parameters θ_{12} , θ_{23} , θ_{13} , Δm_{21}^2 and Δm_{31}^2 are taken as the values from Eq. (26), and the two Majorana CP phases ϕ_1 , ϕ_2 were set to 0.

$\text{BR}(\mu \rightarrow 3e)$.

3.3 Elastic scattering

As we discussed above, there is a unique opportunity at muon colliders to test $C_{LL}^{\mu\mu\mu\mu}$ coefficients by using precision measurements of the angular distribution of elastic $\mu^+\mu^+ \rightarrow \mu^+\mu^+$ scatterings [9]. For this process, there is an interference effect with the SM process of t -channel photon exchange, and therefore the observables depend on $C_{LL}^{\mu\mu\mu\mu}$ linearly rather than $|C_{LL}^{\mu\mu\mu\mu}|^2$. This gives a very good reach in the search for such interactions. It is demonstrated in Ref. [9] that the reach of Λ^{elastic} , which we define as

$$\Lambda^{\text{elastic}} := |C_{LL}^{\mu\mu\mu\mu}|^{-1/2} = \left| \frac{\bar{m}_{\tau\tau}}{\bar{m}_{\mu\mu}} \right| \Lambda \simeq 0.83 \Lambda, \quad (30)$$

is $\Lambda^{\text{elastic}} > 100$ TeV at 2σ C.L. at a $\mu^+\mu^+$ collider with $\sqrt{s} = 2$ TeV and $\mathcal{L} = 120 \text{ fb}^{-1}$, becoming $\Lambda^{\text{elastic}} > 187$ TeV at 90 % C.L. for $\mathcal{L} = 1 \text{ ab}^{-1}$. The reach of Λ^{elastic} translates into $\Lambda > 225$ TeV. Compared with Eqs. (28) and (29), the reach is much higher than the current constraints from the rate muon decays.

In Figure 2, we include the m_1 dependence of the reach of $\Lambda \simeq 1.2\Lambda^{\text{elastic}}$. We see that the reach of this lepton flavor conserving process is stronger than the LFV searches for the whole range of the

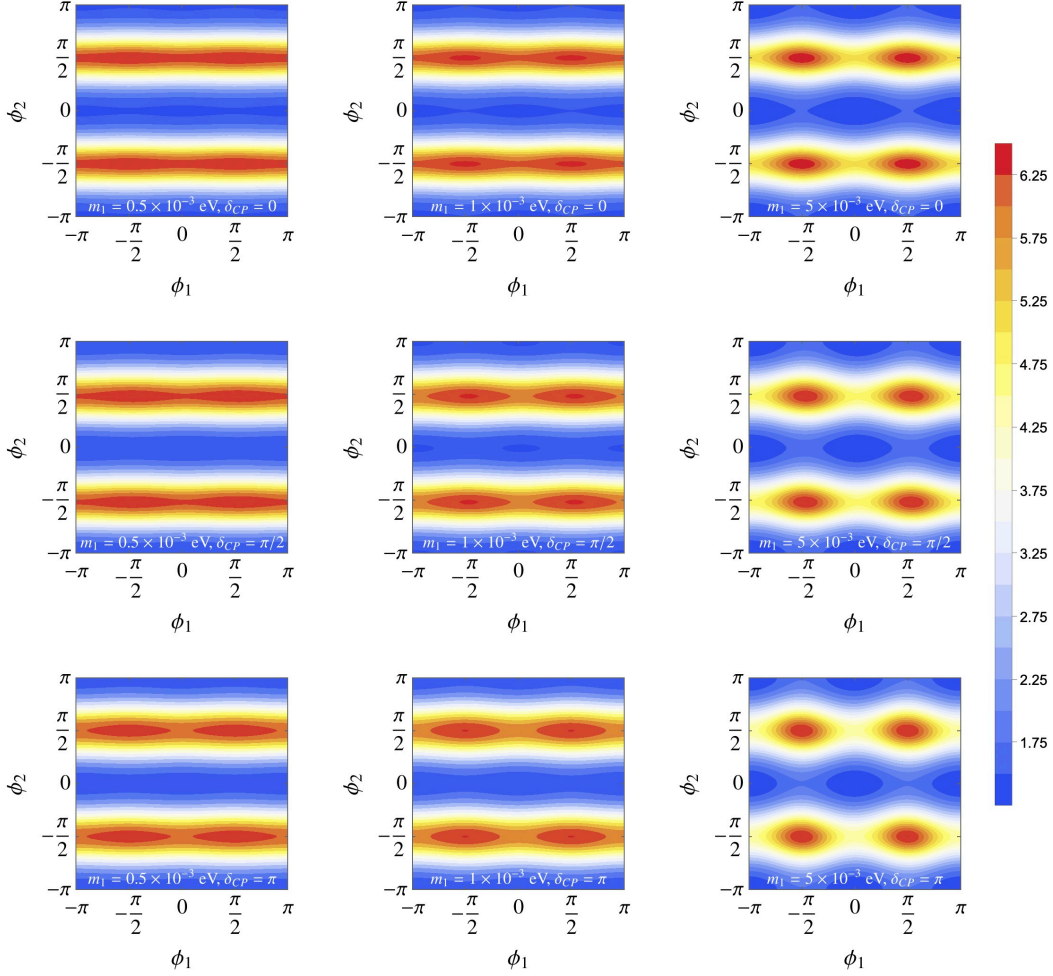


Figure 5: The ratio of cross sections $\sigma(\mu^+\mu^+ \rightarrow \mu^+\tau^+)/\sigma(\mu^+\mu^+ \rightarrow \tau^+\tau^+) = 2|m_{\mu\tau}/m_{\tau\tau}|^2$, as a function of the two Majorana CP-violating phases ϕ_1 and ϕ_2 , for normal mass hierarchy ($m_1 < m_2 < m_3$). The mixing parameters θ_{12} , θ_{23} , θ_{13} , Δm_{21}^2 and Δm_{31}^2 are taken as the values in Eq. (26). The plots on left, middle, and right columns are calculated for $m_1 = 0.5, 1$, and 5 meV, respectively. The plots on top, middle, and bottom rows are calculated for $\delta_{CP} = 0, \pi/2$, and π , respectively.

neutrino masses. This implies that LFV models such as the type-II seesaw could potentially first be discovered as deviations from the SM in elastic processes, and only later appear in LFV observables. However, we emphasize that LFV searches would be needed in order to pinpoint the specific underlying process in case such a deviation is observed.

3.4 Ratios of cross sections

If LFV processes and/or anomalous elastic scatterings are observed, it could be possible to study the flavor structure in LFV coefficients by taking the ratios between different LFV observables. In the

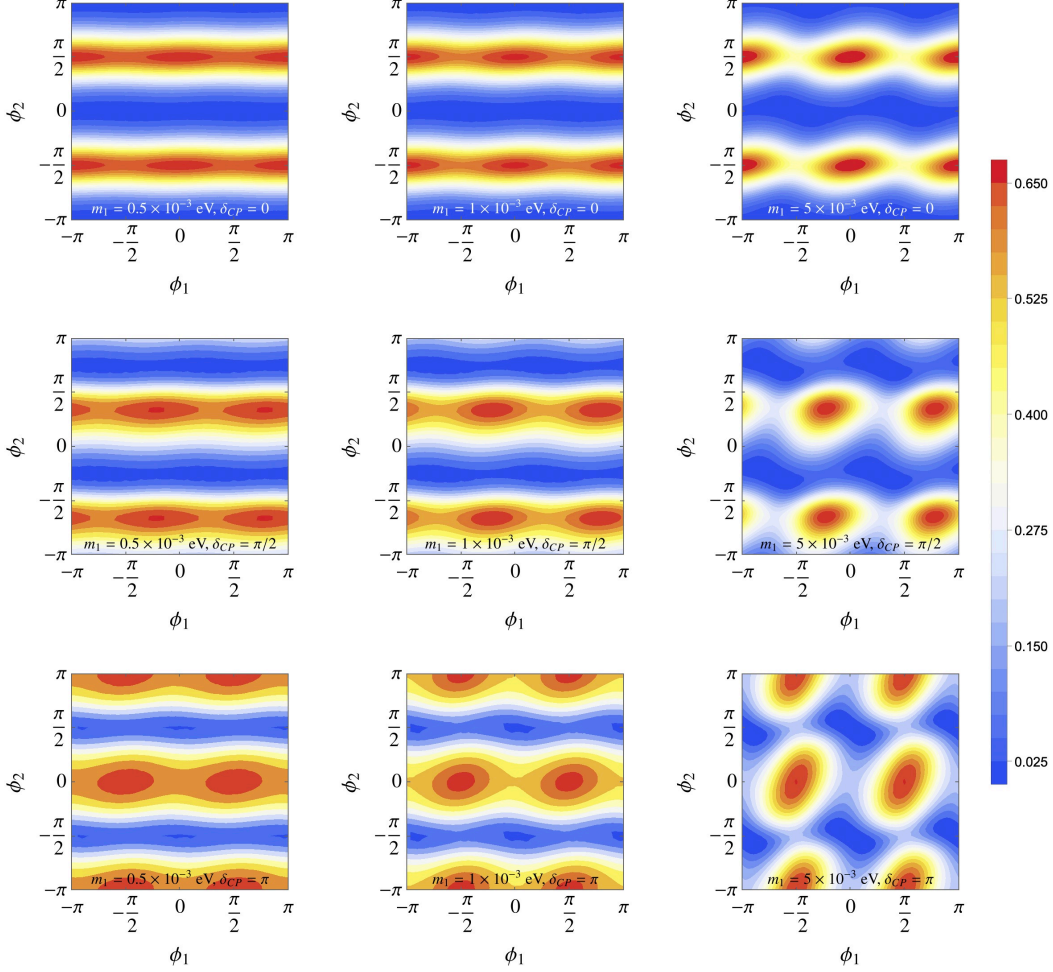


Figure 6: Same as Figure 5 but for $\sigma(\mu^+\mu^+ \rightarrow e^+\tau^+)/\sigma(\mu^+\mu^+ \rightarrow \tau^+\tau^+) = 2|m_{e\tau}/m_{\tau\tau}|^2$.

type-II seesaw model the ratios of LFV cross sections are directly related to neutrino mass matrix, and can therefore be used to cross check the results with neutrino oscillation measurements.

To show such an analysis we here focus on $\mu^+\mu^+ \rightarrow l_i^+\tau^+$ processes with $i = e, \mu$, and τ . In the limit of vanishing external lepton masses, the ratios of cross sections can simply be expressed as

$$\frac{\sigma(\mu^+\mu^+ \rightarrow \mu^+\tau^+)}{\sigma(\mu^+\mu^+ \rightarrow \tau^+\tau^+)} = 2 \left| \frac{m_{\mu\tau}}{m_{\tau\tau}} \right|^2, \quad \frac{\sigma(\mu^+\mu^+ \rightarrow e^+\tau^+)}{\sigma(\mu^+\mu^+ \rightarrow \tau^+\tau^+)} = 2 \left| \frac{m_{e\tau}}{m_{\tau\tau}} \right|^2. \quad (31)$$

In Figure 4 we show these ratios as a function of m_1 and δ_{CP} . We find a strong δ_{CP} dependence in the $e^+\tau^+$ channel, while for the $\mu^+\tau^+$ channel there is mostly only a dependence on m_1 . It would be interesting to check this model prediction with a measurement of δ_{CP} in neutrino oscillation experiments.

In Figures 5 and 6 we show the dependence of the cross section ratios on the Majorana phases ϕ_1

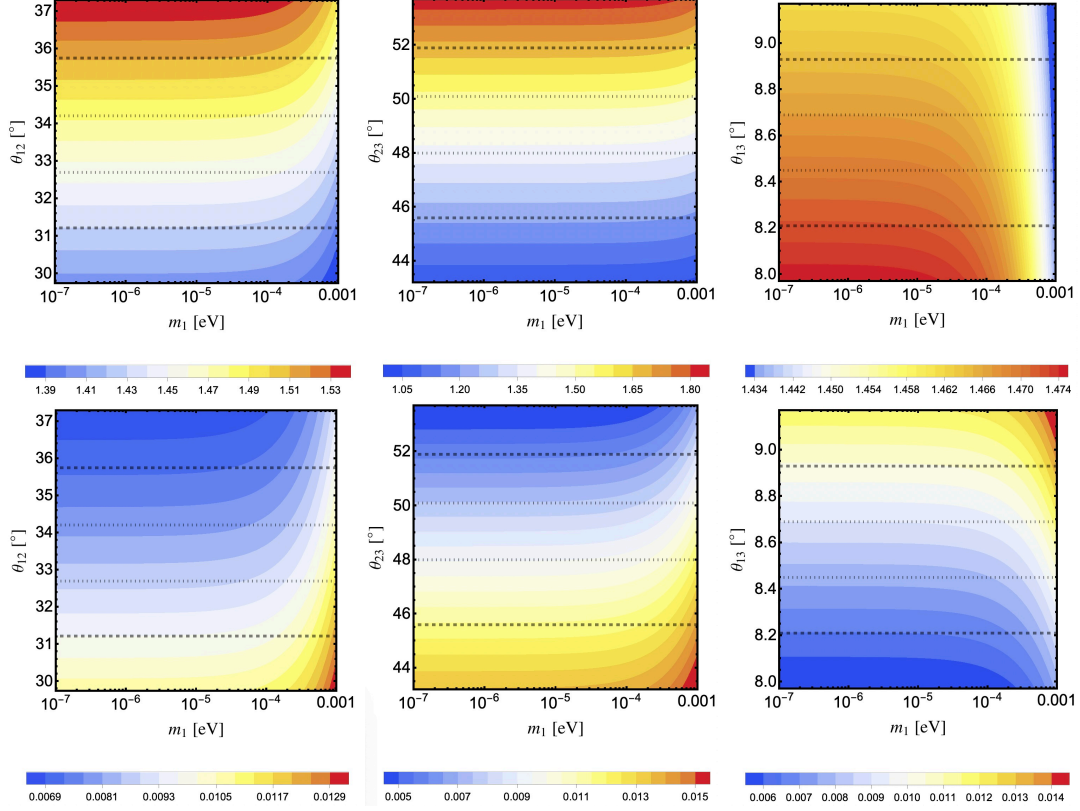


Figure 7: The ratio of cross sections, $\sigma(\mu^+\mu^+ \rightarrow \mu^+\tau^+)/\sigma(\mu^+\mu^+ \rightarrow \tau^+\tau^+)$ (top row) and $\sigma(\mu^+\mu^+ \rightarrow e^+\tau^+)/\sigma(\mu^+\mu^+ \rightarrow \tau^+\tau^+)$ (bottom row) as functions of the lightest neutrino mass m_1 and the mixing parameters θ_{12} (left column), θ_{23} (center column) and θ_{13} (right column). The dotted (dashed) black lines show 1σ (3σ) exclusion lines coming from Ref. [57]. We take the normal hierarchy ($m_1 < m_2 < m_3$) of neutrino masses. The neutrino parameters θ_{12} , θ_{23} , θ_{13} , Δm_{21}^2 and Δm_{31}^2 , unless shown as a parameter along the y -axis, were taken as the values from Eq. (26). The two Majorana CP phases ϕ_1 and ϕ_2 were set to 0.

and ϕ_2 . In each panel, we take different values of m_1 and δ_{CP} . All figures show strong ϕ_2 dependence, and for higher values of m_1 there is also an increasing dependence on ϕ_1 .

The uncertainties associated with the experimental precision of the neutrino mixing angles are shown in Figure 7. We see that the $\mu^+\tau^+$ and $e^+\tau^+$ modes are most sensitive to θ_{23} and θ_{13} , respectively, and with the current experimental precision we have a 30–50% uncertainties in the predictions of the cross section ratios. If the type-II seesaw model would be discovered, $\mu^+\mu^+$ colliders may give one of the most efficient ways to precisely determine the neutrino mixing angles, including CP phases.

4 Summary

One of the primary purposes of a potential future muon collider experiment will be using the high energy reach in direct production searches for new particles. Being a lepton collider, however, it would also enable us to perform precision measurements of Higgs, electroweak, and flavor observables, simultaneously. We demonstrate in this paper the possibilities of searches and studies of LFV processes at $\mu^+\mu^+$ colliders and find that the reach is quite promising.

We study the case with the type-II seesaw model where the LFV interactions are directly related to the neutrino masses and mixings. Firstly, we find that LFV searches at a $\mu^+\mu^+$ collider with $\sqrt{s} = 2$ TeV is as strong as the $\mu \rightarrow e\gamma$ and $\mu \rightarrow 3e$ experiments. Once we combine such searches with the study of precision elastic $\mu^+\mu^+$ scatterings, one can further probe even higher energies or even smaller couplings. We also consider the ratios of LFV cross section as useful quantities to discriminate different models of LFV. These ratios can be expressed in terms of the components in the neutrino mass matrix without additional parameters, and thus one can easily confirm the model predictions.

Of course, during the time at which muon colliders are possible, we should have a good technology of effectively producing and collecting muons. Under such circumstances, new experiments to look for rare muon decays should also be possible with much better sensitivities than those of today, and the discovery may happen first at such experiments. Even in that case, muon colliders are very informative as one can look for many different final states as well as new particles to mediate the LFV process directly to pin down the theory behind LFV and possibly neutrino masses.

Acknowledgements

The work is supported by JSPS KAKENHI Grant Numbers JP19H00689 (RK), JP21H01086 (KF, RK), JP22K21350 (KF, RK), and MEXT KAKENHI Grant Number JP18H05542 (RK).

References

- [1] C. M. Ankenbrandt et al. *Status of muon collider research and development and future plans*. Phys. Rev. ST Accel. Beams 2 (1999), p. 081001. DOI: [10.1103/PhysRevSTAB.2.081001](https://doi.org/10.1103/PhysRevSTAB.2.081001). arXiv: [hep-ph/9901022](https://arxiv.org/abs/hep-ph/9901022).
- [2] M. M. Alsharoa et al. *Recent Progress in Neutrino Factory and Muon Collider Research within the Muon Collaboration*. Phys. Rev. ST Accel. Beams 6 (2003), p. 081001. DOI: [10.1103/PhysRevSTAB.6.081001](https://doi.org/10.1103/PhysRevSTAB.6.081001). arXiv: [hep-ex/0207031](https://arxiv.org/abs/hep-ex/0207031).
- [3] H. Al Ali et al. *The muon Smasher's guide*. Rept. Prog. Phys. 85.8 (2022), p. 084201. DOI: [10.1088/1361-6633/ac6678](https://doi.org/10.1088/1361-6633/ac6678). arXiv: [2103.14043](https://arxiv.org/abs/2103.14043) [[hep-ph](#)].
- [4] J. de Blas et al. *The physics case of a 3 TeV muon collider stage* (2022). arXiv: [2203.07261](https://arxiv.org/abs/2203.07261) [[hep-ph](#)].

- [5] Y. Hamada et al. *μ TRISTAN*. PTEP 2022.5 (2022), 053B02. DOI: [10.1093/ptep/ptac059](https://doi.org/10.1093/ptep/ptac059). arXiv: [2201.06664](https://arxiv.org/abs/2201.06664) [hep-ph].
- [6] C. Accettura et al. *Towards a Muon Collider* (2023). arXiv: [2303.08533](https://arxiv.org/abs/2303.08533) [physics.acc-ph].
- [7] Y. Kondo et al. *Re-Acceleration of Ultra Cold Muon in J-PARC Muon Facility. 9th International Particle Accelerator Conference*. 2018. DOI: [10.18429/JACoW-IPAC2018-FRXGBF1](https://doi.org/10.18429/JACoW-IPAC2018-FRXGBF1).
- [8] S. Weinberg. *A Model of Leptons*. Phys. Rev. Lett. 19 (1967), pp. 1264–1266. DOI: [10.1103/PhysRevLett.19.1264](https://doi.org/10.1103/PhysRevLett.19.1264).
- [9] Y. Hamada et al. *Precision $\mu^+\mu^+$ and μ^+e^- elastic scatterings*. (2022), arXiv: [2210.11083](https://arxiv.org/abs/2210.11083) [hep-ph].
- [10] J. P. Delahaye et al. *Muon Colliders* (2019). arXiv: [1901.06150](https://arxiv.org/abs/1901.06150) [physics.acc-ph].
- [11] M. Abe et al. *A New Approach for Measuring the Muon Anomalous Magnetic Moment and Electric Dipole Moment*. PTEP 2019.5 (2019), p. 053C02. DOI: [10.1093/ptep/ptz030](https://doi.org/10.1093/ptep/ptz030). arXiv: [1901.03047](https://arxiv.org/abs/1901.03047) [physics.ins-det].
- [12] C. A. Heusch and F. Cuypers. *Physics with like-sign muon beams in a TeV muon collider*. AIP Conf. Proc. 352 (1996). Ed. by D. B. Cline, pp. 219–231. DOI: [10.1063/1.49345](https://doi.org/10.1063/1.49345). arXiv: [hep-ph/9508230](https://arxiv.org/abs/hep-ph/9508230).
- [13] P. Minkowski. *$\mu \rightarrow e\gamma$ at a Rate of One Out of 10^9 Muon Decays?* Phys. Lett. B 67 (1977), pp. 421–428. DOI: [10.1016/0370-2693\(77\)90435-X](https://doi.org/10.1016/0370-2693(77)90435-X).
- [14] R. N. Mohapatra and G. Senjanovic. *Neutrino Mass and Spontaneous Parity Nonconservation*. Phys. Rev. Lett. 44 (1980), p. 912. DOI: [10.1103/PhysRevLett.44.912](https://doi.org/10.1103/PhysRevLett.44.912).
- [15] J. Schechter and J. W. F. Valle. *Neutrino Masses in $SU(2) \times U(1)$ Theories*. Phys. Rev. D 22 (1980), p. 2227. DOI: [10.1103/PhysRevD.22.2227](https://doi.org/10.1103/PhysRevD.22.2227).
- [16] T. P. Cheng and L.-F. Li. *Neutrino Masses, Mixings and Oscillations in $SU(2) \times U(1)$ Models of Electroweak Interactions*. Phys. Rev. D 22 (1980), p. 2860. DOI: [10.1103/PhysRevD.22.2860](https://doi.org/10.1103/PhysRevD.22.2860).
- [17] R. N. Mohapatra and G. Senjanovic. *Neutrino Masses and Mixings in Gauge Models with Spontaneous Parity Violation*. Phys. Rev. D 23 (1981), p. 165. DOI: [10.1103/PhysRevD.23.165](https://doi.org/10.1103/PhysRevD.23.165).
- [18] R. Foot et al. *Seesaw Neutrino Masses Induced by a Triplet of Leptons*. Z. Phys. C 44 (1989), p. 441. DOI: [10.1007/BF01415558](https://doi.org/10.1007/BF01415558).
- [19] P. Li, Z. Liu, and K.-F. Lyu. *Heavy neutral leptons at muon colliders*. JHEP 03 (2023), p. 231. DOI: [10.1007/JHEP03\(2023\)231](https://doi.org/10.1007/JHEP03(2023)231). arXiv: [2301.07117](https://arxiv.org/abs/2301.07117) [hep-ph].
- [20] R. Jiang et al. *Searching for Majorana Neutrinos at a Same-Sign Muon Collider* (2023). arXiv: [2304.04483](https://arxiv.org/abs/2304.04483) [hep-ph].
- [21] P. Agrawal et al. *Probing the Type-II Seesaw Mechanism through the Production of Higgs Bosons at a Lepton Collider*. Phys. Rev. D 98.1 (2018), p. 015024. DOI: [10.1103/PhysRevD.98.015024](https://doi.org/10.1103/PhysRevD.98.015024). arXiv: [1803.00677](https://arxiv.org/abs/1803.00677) [hep-ph].
- [22] T. Li and M. A. Schmidt. *Sensitivity of future lepton colliders to the search for charged lepton flavor violation*. Phys. Rev. D 99.5 (2019), p. 055038. DOI: [10.1103/PhysRevD.99.055038](https://doi.org/10.1103/PhysRevD.99.055038). arXiv: [1809.07924](https://arxiv.org/abs/1809.07924) [hep-ph].
- [23] R. Primulando, J. Julio, and P. Uttayarat. *Scalar phenomenology in type-II seesaw model*. JHEP 08 (2019), p. 024. DOI: [10.1007/JHEP08\(2019\)024](https://doi.org/10.1007/JHEP08(2019)024). arXiv: [1903.02493](https://arxiv.org/abs/1903.02493) [hep-ph].
- [24] S. Mandal et al. *Toward deconstructing the simplest seesaw mechanism*. Phys. Rev. D 105.9 (2022), p. 095020. DOI: [10.1103/PhysRevD.105.095020](https://doi.org/10.1103/PhysRevD.105.095020). arXiv: [2203.06362](https://arxiv.org/abs/2203.06362) [hep-ph].
- [25] T. Li, C.-Y. Yao, and M. Yuan. *Revealing the origin of neutrino masses through the Type II Seesaw mechanism at high-energy muon colliders*. JHEP 03 (2023), p. 137. DOI: [10.1007/JHEP03\(2023\)137](https://doi.org/10.1007/JHEP03(2023)137). arXiv: [2301.07274](https://arxiv.org/abs/2301.07274) [hep-ph].

- [26] S. P. Maharathy and M. Mitra. *Type-II see-saw at $\mu^+\mu^-$ collider* (2023). arXiv: [2304.08732 \[hep-ph\]](#).
- [27] W. Rodejohann and H. Zhang. *Higgs triplets at like-sign linear colliders and neutrino mixing*. Phys. Rev. D 83 (2011), p. 073005. DOI: [10.1103/PhysRevD.83.073005](#). arXiv: [1011.3606 \[hep-ph\]](#).
- [28] Y. Cai et al. *Lepton Number Violation: Seesaw Models and Their Collider Tests*. Front. in Phys. 6 (2018), p. 40. DOI: [10.3389/fphy.2018.00040](#). arXiv: [1711.02180 \[hep-ph\]](#).
- [29] P. Bandyopadhyay, A. Karan, and C. Sen. *Discerning Signatures of Seesaw Models and Complementarity of Leptonic Colliders* (2020). arXiv: [2011.04191 \[hep-ph\]](#).
- [30] J.-L. Yang, C.-H. Chang, and T.-F. Feng. *The leptonic di-flavor and di-number violation processes at high energy $\mu^\pm\mu^\pm$ colliders* (2023). arXiv: [2302.13247 \[hep-ph\]](#).
- [31] T. G. Rizzo. *INVERSE NEUTRINOLESS DOUBLE BETA DECAY*. Phys. Lett. B 116 (1982), pp. 23–28. DOI: [10.1016/0370-2693\(82\)90027-2](#).
- [32] D. London, G. Belanger, and J. N. Ng. *New Tests of Lepton Number Violation at Electron - Electron Colliders*. Phys. Lett. B 188 (1987), pp. 155–158. DOI: [10.1016/0370-2693\(87\)90723-4](#).
- [33] W. Rodejohann. *Inverse Neutrino-less Double Beta Decay Revisited: Neutrinos, Higgs Triplets and a Muon Collider*. Phys. Rev. D 81 (2010), p. 114001. DOI: [10.1103/PhysRevD.81.114001](#). arXiv: [1005.2854 \[hep-ph\]](#).
- [34] S. Banerjee et al. *Prospects of Heavy Neutrino Searches at Future Lepton Colliders*. Phys. Rev. D 92 (2015), p. 075002. DOI: [10.1103/PhysRevD.92.075002](#). arXiv: [1503.05491 \[hep-ph\]](#).
- [35] A. G. Akeroyd, M. Aoki, and H. Sugiyama. *Lepton Flavour Violating Decays $\tau \rightarrow \text{anti-}l$ and $\mu \rightarrow e$ gamma in the Higgs Triplet Model*. Phys. Rev. D 79 (2009), p. 113010. DOI: [10.1103/PhysRevD.79.113010](#). arXiv: [0904.3640 \[hep-ph\]](#).
- [36] P. S. Bhupal Dev, R. N. Mohapatra, and Y. Zhang. *Probing TeV scale origin of neutrino mass at future lepton colliders via neutral and doubly-charged scalars*. Phys. Rev. D 98.7 (2018), p. 075028. DOI: [10.1103/PhysRevD.98.075028](#). arXiv: [1803.11167 \[hep-ph\]](#).
- [37] A. Crivellin et al. *Low- and high-energy phenomenology of a doubly charged scalar*. Phys. Rev. D 99.3 (2019), p. 035004. DOI: [10.1103/PhysRevD.99.035004](#). arXiv: [1807.10224 \[hep-ph\]](#).
- [38] P. S. B. Dev et al. *Leptonic scalars and collider signatures in a UV-complete model*. JHEP 03 (2022), p. 068. DOI: [10.1007/JHEP03\(2022\)068](#). arXiv: [2109.04490 \[hep-ph\]](#).
- [39] F. Xu. *Neutral and Doubly-Charged Scalars at Future Lepton Colliders* (2023). arXiv: [2302.08653 \[hep-ph\]](#).
- [40] K. Huitu et al. *Doubly charged Higgs at LHC*. Nucl. Phys. B 487 (1997), pp. 27–42. DOI: [10.1016/S0550-3213\(97\)87466-4](#). arXiv: [hep-ph/9606311](#).
- [41] P. Fileviez Perez et al. *Neutrino Masses and the CERN LHC: Testing Type II Seesaw*. Phys. Rev. D 78 (2008), p. 015018. DOI: [10.1103/PhysRevD.78.015018](#). arXiv: [0805.3536 \[hep-ph\]](#).
- [42] F. del Aguila and J. A. Aguilar-Saavedra. *Distinguishing seesaw models at LHC with multi-lepton signals*. Nucl. Phys. B 813 (2009), pp. 22–90. DOI: [10.1016/j.nuclphysb.2008.12.029](#). arXiv: [0808.2468 \[hep-ph\]](#).
- [43] F. F. Deppisch et al. *Neutrinoless Double Beta Decay and the Baryon Asymmetry of the Universe*. Phys. Rev. D 98.5 (2018), p. 055029. DOI: [10.1103/PhysRevD.98.055029](#). arXiv: [1711.10432 \[hep-ph\]](#).
- [44] F. F. Deppisch, K. Fridell, and J. Harz. *Constraining lepton number violating interactions in rare kaon decays*. JHEP 12 (2020), p. 186. DOI: [10.1007/JHEP12\(2020\)186](#). arXiv: [2009.04494 \[hep-ph\]](#).

- [45] Y. Kuno and Y. Okada. *Muon decay and physics beyond the standard model*. Rev. Mod. Phys. 73 (2001), pp. 151–202. DOI: [10.1103/RevModPhys.73.151](#). arXiv: [hep-ph/9909265](#).
- [46] K. Hayasaka et al. *Search for Lepton Flavor Violating Tau Decays into Three Leptons with 719 Million Produced Tau+Tau- Pairs*. Phys. Lett. B 687 (2010), pp. 139–143. DOI: [10.1016/j.physletb.2010.03.037](#). arXiv: [1001.3221 \[hep-ex\]](#).
- [47] L. Aggarwal et al. *Snowmass White Paper: Belle II physics reach and plans for the next decade and beyond* (2022). arXiv: [2207.06307 \[hep-ex\]](#).
- [48] U. Bellgardt et al. *Search for the Decay $\mu^+ \rightarrow e^+ e^+ e^-$* . Nucl. Phys. B 299 (1988), pp. 1–6. DOI: [10.1016/0550-3213\(88\)90462-2](#).
- [49] K. Arndt et al. *Technical design of the phase I Mu3e experiment*. Nucl. Instrum. Meth. A 1014 (2021), p. 165679. DOI: [10.1016/j.nima.2021.165679](#). arXiv: [2009.11690 \[physics.ins-det\]](#).
- [50] R. L. Workman et al. *Review of Particle Physics*. Prog. Theor. Exp. Phys. 2022 (2022), p. 083C01. DOI: [10.1093/ptep/ptac097](#).
- [51] *Search for doubly charged Higgs boson production in multi-lepton final states using 139 fb⁻¹ of proton-proton collisions at $\sqrt{s} = 13$ TeV with the ATLAS detector* (2022). arXiv: [2211.07505 \[hep-ex\]](#).
- [52] A. M. Baldini et al. *Search for the lepton flavour violating decay $\mu^+ \rightarrow e^+ \gamma$ with the full dataset of the MEG experiment*. Eur. Phys. J. C 76.8 (2016), p. 434. DOI: [10.1140/epjc/s10052-016-4271-x](#). arXiv: [1605.05081 \[hep-ex\]](#).
- [53] B. Aubert et al. *Searches for lepton flavor violation in the decays $\tau^\pm \rightarrow e^\pm \gamma$ and $\tau^\pm \rightarrow \mu^\pm \gamma$* . Physical review letters 104.2 (2010), p. 021802.
- [54] A. Abdesselam et al. *Search for lepton-flavor-violating tau-lepton decays to $\ell \gamma$ at Belle*. JHEP 10 (2021), p. 19. DOI: [10.1007/JHEP10\(2021\)019](#). arXiv: [2103.12994 \[hep-ex\]](#).
- [55] L. Willmann et al. *New bounds from searching for muonium to anti-muonium conversion*. Phys. Rev. Lett. 82 (1999), pp. 49–52. DOI: [10.1103/PhysRevLett.82.49](#). arXiv: [hep-ex/9807011](#).
- [56] P. S. B. Dev, C. M. Vila, and W. Rodejohann. *Naturalness in testable type II seesaw scenarios*. Nucl. Phys. B 921 (2017), pp. 436–453. DOI: [10.1016/j.nuclphysb.2017.06.007](#). arXiv: [1703.00828 \[hep-ph\]](#).
- [57] I. Esteban et al. *The fate of hints: updated global analysis of three-flavor neutrino oscillations*. JHEP 09 (2020), p. 178. DOI: [10.1007/JHEP09\(2020\)178](#). arXiv: [2007.14792 \[hep-ph\]](#).